Published in final edited form as:
Sens Actuators B Chem. 2009 August 18; 141(1): 227–232. doi:10.1016/j.snb.2009.04.034.

Characterization of a novel ultra low refractive index material for biosensor application

Jasenka Memisevic[a], **Venumadhav Korampally**[b], **Shubhra Gangopadhyay**[b], and **Sheila A. Grant**[a,*]

[a] Department of Biological Engineering, University of Missouri, Columbia, MO 65211, USA

[b] Department of Electrical and Computer Engineering, University of Missouri, Columbia, MO 65211, USA

Abstract

Nanoporous materials can provide significant benefits to the field of biosensors. Their size and porous structure makes them an ideal tool for improving sensor performance. This study characterized a novel ultra low index of refraction nanoporous organosilicate (NPO) material for use as an optical platform for fluorescence-based optical biosensors. While serving as the low index cladding material, the novel coating based on organosilicate nanoparticles also provides an opportunity for a high surface area coating that can be utilized for immobilizing biological probes. Biological molecules were immobilized onto NPO, which was spin-coated on silicon and glass substrates. The biological molecule was composed of Protein A conjugated to AlexaFluor 546 fluorophore and then immobilized onto the NPO substrate via silanization. Sample analysis consisted of spectrofluorometry, FT-IR spectroscopy, scanning electron microscopy, contact angle measurement and ellipsometry. The results showed the presence of emission peaks at 574 nm, indicating that the immobilization of Protein A to the NPO material is possible. When compared to Si and glass substrates not coated with NPO, the results showed a 100X and 10X increase in packing density with the NPO coated films respectively. Ellipsometric analysis, FT-IR, contact angle, and SEM imaging of the surface immobilized NPO films suggested that while the surface modifications did induce some damage, it did not incur significant changes to its unique characteristics, i.e., pore structure, wettability and index of refraction. It was concluded that NPO films would be a viable sensor substrate to enhance sensitivity and improve sensor performance.

Keywords

nanoporous material; biosensor; protein immobilization

1. Introduction

Optical biosensors have had numerous uses since their discovery in 1960s [1]. The most important performance parameters of optical biosensors are specificity and signal intensity. Researchers have been attempting to enhance sensitivity by using new materials as biosensor

*Corresponding author; E-mail: grantsa@missouri.edu, Address: 250 Ag. Engineering Building, University of Missouri, Columbia, MO 65211, USA. Telephone: 573-884-9666. Fax: 573-882-1115.

platforms [2,3]. Recently, porous materials have been under investigations for the benefit of signal intensity enhancement through increased surface area available for binding. Several studies have evaluated the use of porous, nanoporous, and mesoporous materials for both label free [4–6] and fluorescence-based [7–9] optical biosensors. The label-free sensors rely on detection of refractive index change upon analyte binding. A nanoporous structure allows more sensitivity in this detection due to the relationship between surface structure and analyte sizes. On the other hand, fluorescence biosensors detect analytes by observing analyte-induced changes in fluorescence. The performance of a fluorescence biosensor depends on its ability to guide light, and a nanoporous structure greatly aids in this task.

The increasing interest in porous materials is related to the ability of the porous structure to provide a low refractive index for fluorescence-based biosensors and a better surface feature-to-analyte size ratio for label-free sensors. For fluorescence sensors, a lower refractive index of sensor platform permits the use of liquid core waveguides (LCWs). LCWs in turn provide more fluorescence generation and capture due to the fact that the fluorophore excitation source is not evanescently based. Therefore, by using a nanoporous substrate material in a fluorescence biosensor, benefits can be gained from both increased immobilization and direct, in-solution excitation.

Several groups have reported the use of low refractive index materials in LCW biosensors [10–12]. Recently, a series of amorphous copolymers of polytetra-fluoroethylene (PTFE) with 2,2-bis- (trifluoromethyl)-4,5difluoro-1,3 dioxole (Teflon AF) has attracted considerable interest in microfluidic applications [13–15]. They are essentially transparent throughout 200 to 2000 nm wavelength range with refractive index 1.29 to 1.31, lower than that of water (n=1.33). Thus, when such material is solution cast or spin-coated into several microns thin film on a capillary or microchannel and water is allowed to pass, it behaves as a LCW and can effectively transfer light launched at one end to another. There are a number of reports on LCWs based on plastic and glass capillaries coated internally with Teflon-AF [16–19], glass capillaries coated externally with Teflon-AF [12,20–23] and capillaries made entirely of Teflon [24–32]. Gangopadhyay and her group, for the first time, reported about fabrication and characterization of a chip-based Teflon-AF coated liquid core waveguide on Si and glass [10,33,34]. Using Teflon-AF as a coating inside glass capillaries, they were able to fabricate low-loss optical waveguide microchannels. However, Teflon-AF is very hydrophobic and resistant to adhesion making it difficult to use with microfabricated channels on Si. The process of coating surfaces with Teflon-AF is tedious and lengthy, as it requires multiple patterning, etching, and bonding steps.

We report on the characterization of a novel, low index of refraction (RI), nanoporous material as a biosensor substrate. Experiments were performed to evaluate the possibility of immobilizing biological molecules onto the NPO surface without incurring material changes during modification steps necessary for biosensor immobilization. Experiments using surface analysis tools such as fluorescence spectroscopy, ATR FT-IR, ellipsometry, scanning electron microscopy (SEM), and contact angle determined that although various modifications steps incurred some changes in the material's surface properties, they did not significantly alter its usability in fluorescence biosensors. The use of NPO as a platform for fluorescence biosensors is evaluated, with specific application in liquid core waveguides.

2. Materials and Methods

2.1. NPO Fabrication and Spin Coating

The proprietary NPO solution protocol was developed by and adopted from Gangopadhyay's group. Substrates were prepared for coating by cleaning with acetone, isopropanol, and methanol, and dried with air. Clean Si wafer and borosilicate glass substrates were placed on

a spin coater, several drops of NPO were suspended on the top surface, spun at 3000 rpm for 30 seconds. Finally, silicon and glass substrates were baked on a hot plate or in a furnace, respectively, at 470°C for at least 5 minutes.

2.2. Surface Silanization

Surfaces coated with NPO have previously been characterized and determined to consist of predominantly methyl groups [35]. In order to perform silanization, methyl groups from the surfaces were replaced with silanol (Si-OH) groups by oxygen-plasma treatment with an Applied Materials Precision 5000 PECVD at 12 watts for 20 seconds. After the plasma treatment, samples were placed in water for 5 minutes. The silanization procedure closely followed one by Bhatia [36], with the initial water boiling and acid cleaning steps omitted. The cleaning was omitted in order to avoid damage to the NPO coat. Samples were assumed to be sufficiently clean due to the fact that Si and glass substrates were cleaned prior to NPO coating and the coating was performed in a Class 100 clean room. Briefly, NPO-coated samples were incubated in 2% (3-Mercaptopropyl)trimethoxysilane (MTS, Fluka) in Toluene (Sigma, St. Louis, MO) (v/v) solution, for 1–1.5 hrs in a Nitrogen bag, washed in Toluene for 3 minutes, and dried with Nitrogen gas. Next, 5 mM MaleimidoButyryloxy-Succinimide ester (GMBS, Pierce, Rockford, IL) in Ethanol (Sigma, St. Louis, MO) was placed on top of the samples for 1 hour, after which the samples were washed 3X with Phosphate Buffered Saline (PBS, Sigma, St. Louis, MO). GMBS was dissolved in approximately 50μl N,N-Dimethylformamide (DMF, Fluka) before adding to ethanol. Precautions were taken to prevent ethanol from drying during incubation.

2.3. Biological Immobilization

After the samples were silanized, Protein A conjugated to Alexa Fluor 546 (AF546, Invitrogen), was immobilized to the surfaces. The immobilization procedure was adopted from Bhatia [36] with modifications. Protein A conjugated to AF546 was mixed with PBS to obtain a desired protein concentration of 35 μg/ml. Proteins were placed on top of each sample wafer, using surface tension to hold solution in place, and incubated overnight at 4°C. After incubation, the protein solution was removed and samples washed 3X with PBS, and replaced with 3% Bovine Serum Albumin (BSA, Sigma, St. Louis, MO) solution. After 1-hour incubation, samples were washed again using the procedure described above.

2.4. Fluorescence Measurements and Data Analysis

A vertical, flat sample holder was used in the FluoroMax-3 spectrofluorometer (Yvon Jobin), to measure fluorescence. The sample holder was oriented at 33° relative to the detector, as it was previously determined that light collection was most efficient at that position. Samples were consistently kept in a PBS bath and measurements were obtained immediately upon removal from the liquid environment. This ensured that the samples were wet throughout measurements, which closely resembles conditions in a liquid-core waveguide biosensor. All samples were excited at 546nm wavelength, at 0.3s integration, and 5nm slits.

2.5. ATR FT-IR Measurement

Attenuated Total Reflection Fourier Transform – Infra Red (ATR FT-IR) spectra were obtained from Si/NPO samples, using Si blank samples as controls. All measurements were obtained using Nicolet FT-IR spectrometer (ThermoFisher) with OMNIC software. Samples were placed on top of the attenuated total reflectance (ATR) crystal and pressure was applied mechanically until sufficient contact was made with the diamond crystal. Background spectra were obtained from ambient air. Data collection was averaged over 64 runs and the background spectrum was subtracted. In order to preserve all original peaks, baseline correction was not performed.

2.6. SEM Imaging and Characterization

Samples were prepared for Scanning Electron Microscopy (SEM) by placing them on a plain Al SEM stub with adhesive Carbon tape, using Silver paint to ground electrons. Secondary electrons were captured with the Everhart-Thornley detector in a Quanta SEM (FEI) with a low vacuum setting. Two types of samples were imaged for subsequent comparison, Si/NPO substrates and Si/NPO substrates with surface modification by silanization and crosslinking. Images of both sample types were obtained under the same magnification, beam current, beam energy, and chamber pressure in order to ensure proper comparison.

2.7. Contact Angle Measurements

Materials used as biosensor platforms need to possess a hydrophilic surface that allows biomolecule attachment. Oxygen/plasma coating treatment can be utilized to eliminate hydrophobicity of NPO. In order to immobilize biological molecules, the surface has to be silanized and crosslinked, while maintaining its hydrophilic nature. Wettability experiments were performed on modified Si/NPO surfaces using the sessile drop technique. Surfaces were examined after silanization and application of the crosslinker, as well as after protein immobilization. Results were compared to those previously obtained for unmodified Si/NPO.

2.8. Refractive Index Measurement

For use in liquid core waveguide- based biosensors, the refractive index of NPO must remain below that of water (n=1.33). While the pores are present on surface of Si after NPO is spin coated, ellipsometry was used to determine whether the refractive index changes after silanization and crosslinking steps are performed. J. A. Woollam V.A.S.E. ellipsometer was used to calculate the refractive index of plain Si/NPO samples, as well as the silanized and crosslinked Si/NPO samples. Data fitting was performed using Cauchy layer method and the refractive index was obtained for each layer.

3. Results and Discussion

3.1. Biological immobilization and fluorescence collection

Si wafers and borosilicate glass substrates were coated with NPO, and Protein A/AF546 was immobilized to their surfaces. The resulting substrates were placed in a FluoroMax-3 spectrofluorometer, excited with 546 nm light, and the fluorescence emission was captured. For statistical repeatability purposes, three separate samples of each type were tested with and without NPO, as seen in Fig. 1. It is clear that the fluorescence of Protein A/AF546 immobilized to both Si and glass samples coated and not coated with NPO had significantly differing intensities. The presence of emission peak at 574 nm signifies that Protein A has been successfully immobilized to the NPO surface and the AF 546 dye is emitting light. It can be seen that while the emission fluorescence intensity from Si samples without NPO is in the tens of thousands counts range, those from Si samples with NPO coating are in the several million counts range. Specifically, the observed change in intensity was from 50K–100K cps without NPO to 2.75M–3.75M cps with NPO. Similarly, on glass samples the fluorescence intensity change was more than 1 million counts. Glass samples without NPO had about 300K counts and samples with NPO had 1–2M counts. This suggests that the NPO coat has a fluorescence enhancement characteristic, where the fluorescence intensity in this study was enhanced up to a hundred times on Si and up to ten times on glass by using NPO. We attribute this result to the porous nature of NPO, which creates a larger overall surface area for binding of Protein A. While porous silicon also provides fluorescence enhancement, it has been shown that the thickness of the porous film is proportional to the fluorescence intensity [7]. Due to the fact that the pores are an inherent part of NPO, this suggests that it provides a much simpler method of fabricating a biosensor platform compared to the time required to generate pores in Si. To

further determine if the porous nature of NPO is causing the fluorescence enhancement, results were compared to those of non-porous coating. Namely, Si substrates were coated with non-porous poly(methylsilsesquioxane) PMSSQ. The results shown in Fig. 2, suggest that non-porous PMSSQ does increase fluorescence somewhat as compared to plain Si substrates.

However, the samples with porous NPO still produced the greatest fluorescence intensities. The increase of surface area for biomolecular immobilization has been reported before for mesoporous materials [37]. We have performed size calculations for Protein A and determined that it is approximately equal to the average pore size of about 5nm. However, while it appears that surface area increase due to porosity could not be attributed to the fluorescence enhancement by Protein A alone, it could be due to the presence of the heterobifunctional crosslinker, GMBS. Namely, while Protein A is immobilized to the NPO, it is not directly attached to its surface. The crosslinker GMBS acts as an intermediate between NPO and Protein A. GMBS consists of a long, chain-like structure where one end binds to NPO and the other end binds Protein A. Silanization of NPO with MTS introduces thiol groups to the inside and outside of the pores, and GMBS binds the thiol groups. Therefore, GMBS has the opportunity to bind in multiple locations inside of a nanopore and extend its chains out of the pore to bind Protein A. Hence, a benefit from the increased surface area created by the pores is still obtained. The limitations of this system are encountered at the point where the immobilization at the surface is maximal due to steric hindrance between proteins bound to GMBS in close proximity to each other.

While the increase in fluorescence with NPO is evident, there are also variations between samples with the same treatment, i.e. with and without NPO. These variations can be attributed to the inconsistent sample size and thus variable overall Protein A/AF546 solution volume. Another source of variation could be equipment error introduced by pipetting small volumes.

3.2. ATR FT-IR analysis

Since NPO on silicon demonstrated the highest binding sites and fluorescence, additional tests were performed. In order to ensure that silanization and crosslinking were successfully accomplished without altering the properties of NPO, ATR FT-IR spectroscopy was performed on Si/NPO samples before and after silanization and crosslinking. Fig. 3 shows the resulting ATR FT-IR scans of Si/NPO surface with observable Si and OH peaks. A representative scan of a Si/NPO surface after silanization and crosslinking is shown on the same graph. In both sample types, there is a CH_3 vibration peak at 2930 cm^{-1}, CH_3 vibration peak at 2855 cm^{-1}, and an OH peak at 3400 cm^{-1}. Previously published studies on FT-IR spectra of MTS silanized silicon-based surfaces have also reported the same peaks [38,39], even with porous surfaces [40]. According to the NPO spectra, these peaks are present before and after silanization, suggesting that the surface chemistry already contains CH_3. While it appears that the two sample types have the same surface chemistries that does not mean that silanization did not occur. This is attributed to the fact that, according to ellipsometry measurements, the silanized layer is much thinner than the penetration depth of ATR FT-IR sampling. As expected, the differences in the surface chemistries between the two samples are too small to be specifically detected. However, the FT-IR spectra demonstrated that the silanization and crosslinking procedures did not significantly alter the NPO chemistry.

3.3. SEM imaging results

Immobilization of Protein A to the surface of NPO-coated substrates required several surface modification steps, such as oxygen/plasma coating, silanization, and application of heterobifunctional groups. While the purpose of these steps was to modify the functional groups present on the surface, a possibility of physical change was present. SEM was utilized to verify that no substantial damage was incurred to NPO on functionalized substrates. Fig. 4 shows

SEM images of Si substrate coated with NPO before and after functionalization. These images suggest that the gross structure seen on surface of unmodified Si/NPO substrate is also seen in the modified Si/NPO substrate. Therefore, the treatments performed to modify Si/NPO surfaces did not change the overall physical characteristics, as compared to unmodified NPO samples.

3.4. Contact angle measurements

Previous work determined that the NPO surface was hydrophobic, having a contact angle of 95–100°. The results of contact angle measurements after surface modifications show that Si/NPO surfaces treated with oxygen/plasma, silanization and crosslinking had a contact angle of about 30°. This suggests that the samples have become hydrophilic. Furthermore, subsequent immobilization of biological molecules increased the contact angle to about 45°, which remains much lower than of the untreated, hydrophobic surface. The results obtained here are comparable to those reported for the more commonly used porous silcon, which has a contact angle of 20° when functionalized with acrylic acid and 120° when functionalized with decene [8]. Liquid core waveguide biosensors should allow liquid to easily fill the waveguide channels, and our results suggest that this can be achieved even after biomolecule immobilization to NPO.

3.5. Refractive index measurements

Ellipsometry was utilized to determine whether the refractive index changes due to the silanization and crosslinking surface modifications. The refractive index calculated for NPO spin coated onto Si wafer substrates was 1.17 at 630 nm light wavelength. Subsequent measurement of refractive index of NPO/Si samples with a modified surface yielded insightful results. The samples were modeled as having two layers created by the NPO coating and surface modifications (oxygen/plasma treatment, silanization, crosslinking, and immobilization). Different sample types were measured: 1) NPO with silanization, 2) NPO with silanization, crosslinking, and immobilization, and 3) plain NPO samples. The results, shown in Table 1, suggest that the refractive index increases in the layer created by the oxygen/plasma and immobilization coating to 1.46, while the underlying NPO layer remains ultra-low at 1.17–1.19.

The increase in the refractive index of oxygen treated surface from 1.17 to 1.28 indicates that the top layer was altered by the plasma treatment. There are two possible reasons for the change in the index of refraction: 1) damage of the top layer and loss of porosity and/or 2) removal of CH_3 and incorporation of OH. However, it was also determined that the thickness of the oxygen/plasma layer is 15–30nm, which is still much smaller than the wavelength of incident light used in a biosensor. Thus, a very thin damaged layer should not hinder the light guiding abilities of the NPO films.

On the other hand, a damaged surface layer and loss of porosity should not show an increase in binding site, but fluorescence data showed a very large enhancement of fluorescence. This can be explained by the damaged top layer resulting in a rough surface topography, which increased binding sites. Also, increased OH groups would enhance the binding sites and thus enhance fluorescence.

Therefore, although a significant increase in the refractive index of 0.11 in the NPO layer was observed between modified and unmodified samples, the damaged layer was extremely thin and should not hinder the light guiding ability. Also, even with the increase, the refractive index remains much lower than that of water, making them appropriate for use in liquid core waveguide in microfluidic chips. Most importantly, the NPO films demonstrated increased fluorescence, which will translate to enhanced sensor performance. These results further confirm that NPO is a suitable surface for biosensor applications.

4. Conclusions

Nanoporous organosilicate material was characterized for its potential use as a biosensor substrate. Particular interest for this material could be found in liquid-core waveguide biosensors. A comprehensive study involving fluorescence measurements, FT-IR, SEM imaging, refractive index measurement, and contact angle measurements before and after surface modifications was completed. The results suggest that NPO is indeed a good candidate for fluorescent biosensors due to the fluorescence enhancement provided by increased surface area. Additionally, it has an ultra-low refractive index, lower than that of water, making it feasible for use as a microchannel coating in liquid-core waveguides. While other materials with refractive indices lower than that of water exist, such as Teflon AF, they have difficulty adhering to other materials. NPO, on the other hand, can be easily spin coated to a waveguide surface and stored at room temperature until future use. Future work includes incorporating NPO into a liquid core waveguides, for fast, reliable, and sensitive detection of antibody based fluorescent biosensors.

Acknowledgments

The authors would like to thank Lou Ross for his assistance in obtaining SEM images and Greg Pribil at J. A. Woollam for assistance with ellipsometry data analysis, and Richard C. Stringer for assistance in ellipsometry data collection.

References

1. Clark LC, Lyons C. Electrode systems for continuous monitoring in cardiovascular surgery. Annals of the New York Academy of Sciences 1962;102:29–45. [PubMed: 14021529]
2. Himmelhaus M, Takei H. Cap-shaped gold nanoparticles for an optical biosensor. Sensors and Actuators B: Chemical 2000;63:24–30.
3. Vo-Dinh T, Cullum BM, Stokes DL. Nanosensors and biochips: Frontiers in biomolecular diagnostics. Sensors and Actuators B: Chemical 2001;74:2–11.
4. Bonanno LM, DeLouise LA. Whole blood optical biosensor. Biosensors and Bioelectronics 2007;23:444–448. [PubMed: 17720473]
5. Di Francia G, Ferrara VL, Manzo S, Chiavarini S. Towards a label-free optical porous silicon DNA sensor. Biosensors and Bioelectronics 2005;21:661–665. [PubMed: 16202880]
6. Vaseashta A, Dimova-Malinovska D. Nanostructured and nanoscale devices, sensors and detectors. Science and Technology of Advanced Materials 2005;6:312–318.
7. Risk W, Kim H, Miller R, Temkin H, Gangopadhyay S. Optical waveguides with an aqueous core and a low-index nanoporous cladding. Optics Express 2004;12:6446–6455. [PubMed: 19488295]
8. Rossi A, Wang L, Reipa V, Murphy TE. Porous silicon biosensor for detection of viruses. Biosensors and Bioelectronics 2007;23:741–745. [PubMed: 17723292]
9. Wolfbeis OS, Oehme I, Papkovskaya N, Klimant I. Sol-gel based glucose biosensors employing optical oxygen transducers, and a method for compensating for variable oxygen background. Biosensors and Bioelectronics 2000;15:69–76. [PubMed: 10826645]
10. Manor R, Datta A, Ahmad I, Holtz M, Gangopadhyay S, Dallas T. Microfabrication and characterization of liquid core waveguide glass channels coated with Teflon AF. IEEE Sensors Journal 2003;3:687–692.
11. Dasgupta PK, Genfa Z, Li J, Boring CB, Jambunathan S, Al-Horr R. Luminescence detection with a liquid core waveguide. Analytical Chemistry 1999;71:1400–1407.
12. Hanning A, Lindberg P, Westberg J, Roeraade J. Laser-induced fluorescence detection by liquid core waveguiding applied to DNA sequencing by capillary electrophoresis. Analytical Chemistry 2000;72:3423–3430. [PubMed: 10952522]
13. Ding SJ, Wang PF, Zhang DW, Wang JT, Lee WW. A novel structural amorphous fluoropolymer film with an ultra-low dielectric constant. Materials Letters 2001;49:154–159.
14. Lowry JH, Mendlowitz JS, Subramanian NS. Optical characteristics of Teflon AF fluoroplastic materials. Optical Engineering 1992;31:1982–1985.

15. DuPont. Teflon AF properties. 2007
16. Dress P, Franke H. A cylindrical liquid-core waveguide. Applied Physics B: Lasers and Optics 1996;63:12–19.
17. Dress, P.; Franke, H. Optical fiber with a liquid H_2O core; SPIE Integrated Optics and Microstructures Conference; San Jose, CA, USA. 1996.
18. Dress P, Franke H. Increasing the accuracy of liquid analysis and pH-value control using a liquid-core waveguide. Review of Scientific Instruments 1997;68:2167–2171.
19. Hong, K.; Burgess, LW. Liquid-core waveguides for chemical sensing; SPIE Chemical, Biochemical and Environmental Fiber Sensors VI Conference; San Diego, CA, USA. 1994.
20. Altkorn R, Koev I, Gottlieb A. Waveguide capillary cell for low-refractive-index liquids. Applied Spectroscopy 1997;51:1554–1558.
21. Curcio M, Stålhandske P, Lindberg P, Roeraade J. Multiplex high-throughput solid-phase minisequencing by capillary electrophoresis and liquid core waveguide fluorescence detection. Electrophoresis 2002;23:1467–1472. [PubMed: 12116157]
22. Dasgupta PK, Genfa Z, Poruthoor SK, Caldwell S, Dong S, Liu SY. High-sensitivity gas sensors based on gas-permeable liquid core waveguides and long-path absorbance detection. Analytical Chemistry 1998;70:4661–4669.
23. Wang SL, Huang XJ, Fang ZL, Dasgupta PK. A miniaturized liquid core waveguide-capillary electrophoresis system with flow injection sample introduction and fluorometric detection using light-emitting diodes. Analytical Chemistry 2001;73:4545–4549. [PubMed: 11575805]
24. Altkorn R, Koev I, Van Duyne RP, Litorja M. Low-loss liquid-core optical fiber for low-refractive-index liquids: Fabrication, characterization, and application in Raman spectroscopy. Applied Optics 1997;36:8992–8998. [PubMed: 18264455]
25. Gooijer C, Hoornweg GP, De Beer T, Bader A, Van Iperen DJ, Brinkman UAT. Detector cell based on plastic liquid-core waveguides suitable for aqueous solutions: One-to-two decades improved detection limits in conventional-size column liquid chromatography with absorption detection. Journal of Chromatography A 1998;824:1–5.
26. Larsson H, Dasgupta PK. Liquid core waveguide-based optical spectrometry for field estimation of dissolved BTEX compounds in groundwater: A feasibility study. Analytica Chimica Acta 2003;485:155–167.
27. Li Q, Morris KJ, Dasgupta PK, Raimundo IM, Temkin H. Portable flow-injection analyzer with liquid-core waveguide based fluorescence, luminescence, and long path length absorbance detector. Analytica Chimica Acta 2003;479:151–165.
28. Liu Z, Pawliszyn J. Capillary isoelectric focusing of proteins with liquid core waveguide laser-induced fluorescence whole column imaging detection. Analytical Chemistry 2003;75:4887–4894. [PubMed: 14674468]
29. Song L, Liu S, Zhelyaskov V, El-Sayed MA. Application of liquid waveguide to Raman spectroscopy in aqueous solution. Applied Spectroscopy 1999;52:1364–1367.
30. Tanikkul S, Jakmunee J, Rayanakorn M, Grudpan K, Marquardt BJ, Gross GM, Prazen BJ, Burgess LW, Christian GD, Synovec RE. Characterization and use of a Raman liquid-core waveguide sensor using preconcentration principles. Talanta 2003;59:809–816. [PubMed: 18968968]
31. Waterbury RD, Yao W, Byrne RH. Long pathlength absorbance spectroscopy: Trace analysis of Fe (II) using a 4.5 m liquid core waveguide. Analytica Chimica Acta 1997;357:99–102.
32. Yao W, Byrne RH. Determination of trace chromium(VI) and molybdenum(VI) in natural and bottled mineral waters using long pathlength absorbance spectroscopy (LPAS). Talanta 1999;48:277–282. [PubMed: 18967465]
33. Datta A, In-Yong E, Dhar A, Kuban PA, Manor RA, Ahmad IA, Gangopadhyay SA, Dallas TA, Holtz MA, Temkin HA, Dasgupta PK. Microfabrication and characterization of Teflon AF-coated liquid core waveguide channels in silicon. IEEE Sensors Journal 2003;3:788–795.
34. Manor, R.; Datta, A.; Dhar, A.; Holtz, MA.; Berg, JA.; Gangopadhyay, SA.; Dasgupta, PA.; Temkin, HA.; Veeraraghavan, VA.; Vijayaraghavan, RA.; Dallas, TA. Microfabricated liquid core waveguides for microanalysis systems; IEEE Conference; 2002.

35. Lubguban AA, Lubguban JA, Othman MT, Shende RV, Gangopadhyay S, Miller RD, Volksen W, Kim HC. Supercritical CO2/co-solvent extraction of porogens and surfactant templates to obtain ultralow dielectric constant films. Thin Solid Films 2008;516:4733–4741.

36. Bhatia SK, Shriver-Lake LC, Prior KJ, Georger JH, Calvert JM, Bredehorst R, Ligler FS. Use of thiol-terminal silanes and heterobifunctional crosslinkers for immobilization of antibodies on silica surfaces. Analytical Biochemistry 1989;178:408–413. [PubMed: 2546467]

37. Xu Q, Zhu JJ, Hu XY. Ordered mesoporous polyaniline film as a new matrix for enzyme immobilization and biosensor construction. Analytica Chimica Acta 2007;597:151–156. [PubMed: 17658325]

38. Mansur H, Oréfice R, Pereira M, Lobato Z, Vasconcelos W, Machado L. FTIR and UV-Vis study of chemically engineered biomaterial surfaces for protein immobilization. Spectroscopy: An International Journal 2002;16:351–360.

39. Coman V, Grecu R, Wegmann J, Bachmann S, Albert K. Solid-state NMR and FTIR characterization of 3-mercaptopropyl silica gel R. Physica Special Issue 2001:326–331.

40. Yantasee W, Lin Y, Li X, Fryxell GE, Zemanian TS, Viswanathan VV. Nanoengineered electrochemical sensor based on mesoporous silica thin-film functionalized with thiol-terminated monolayer. The Analyst 2003;128:899–904.

Biographies

Jasenka Memisevic obtained the BS degree in biomedical engineering from Saint Louis University in 2006.

As an undergraduate, she performed research in a Tissue Engineering laboratory at Saint Louis University for 2 years. She also completed a National Science Foundation's Research Experience for Undergraduates program at The Johns Hopkins University. She is currently working for her Ph.D. degree at the Biosensors and Biomaterials Laboratory of University of Missouri. She is also National Science Foundation's Graduate Research Fellow.

Venumadhav Korampally received the B.S degree in electrical engineering from Kakatiya University, India in 2000 and M.S and Ph.D. degrees in electrical engineering from University of Missouri in 2004 and 2007, respectively. He is currently working as a postdoctoral research associate at the University of Missouri.

His current research interests include ultra low refractive index films for optofluidic biosensors, nanoparticles for bioimaging and drug delivery.

Shubhra Gangopadhyay received the Ph.D. degree in physics from the Ingian Institute of Technology, Kharagpur, in 1982. From 1983 to 1985, she was a Visiting Scientist at Universitat Kaiserslautern, Germany, working on semiconductor physics. Since 1985, she has been with the Department of Physics, Texas Tech University, Lubbock, working in the areas of material science, semiconductor device physics, microelectronics, and microsensors. She joined the University of Missouri, Columbia, in the fall of 2003 as a LaPierre Chair Professor, Department of Electrical Engineering.

Dr. Gagopadhyay's research interest include BioMEMS, nanoenergetics, PECVD, evaporation, and sputtering deposition of thin-film dielectrics, amorphous silicon, carbon, and silicon carbide films, as well as ellipsometry, UV-vis, FT-IR, and current-voltage/capacitance voltage device characterization.

Sheila A. Grant received her Ph.D. degree in Materials Science and Engineering and MS degree in Biomedical Engineering from Iowa State University. After graduation, she worked as a research engineer at Lawrence Livermore National Laboratory in Livermore, CA for four years.

Currently, she is an associate professor in the Department of Biological Engineering at the University of Missouri. Grant's research interests involve developing novel sensing mechanisms and sensing platforms by utilizing new advances in microtechnology and nanotechnology to improved sensitivity, miniaturization, portability, and low cost. Additionally, she is developing nanostructured composites for soft and hard tissue repair. She holds two patents and numerous disclosures.

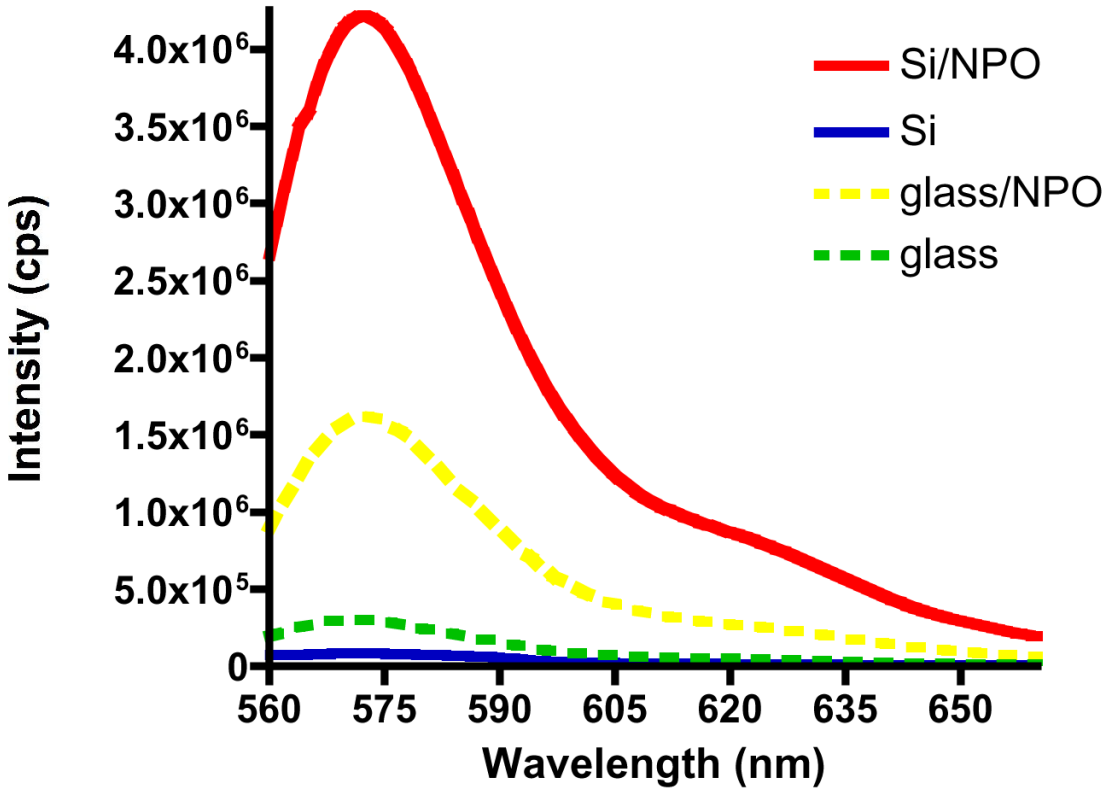

Fig. 1.

Fluorescence emission from immobilized ProteinA/AF546 on Si and glass samples in presence and absence of NPO coating. Si/NPO – Silicon substrate coated with NPO (red), Si – Silicon substrate not coated with NPO (blue), glass/NPO – glass substrate coated with NPO (dotted yellow), glass – glass substrate not coated with NPO (dotted green).

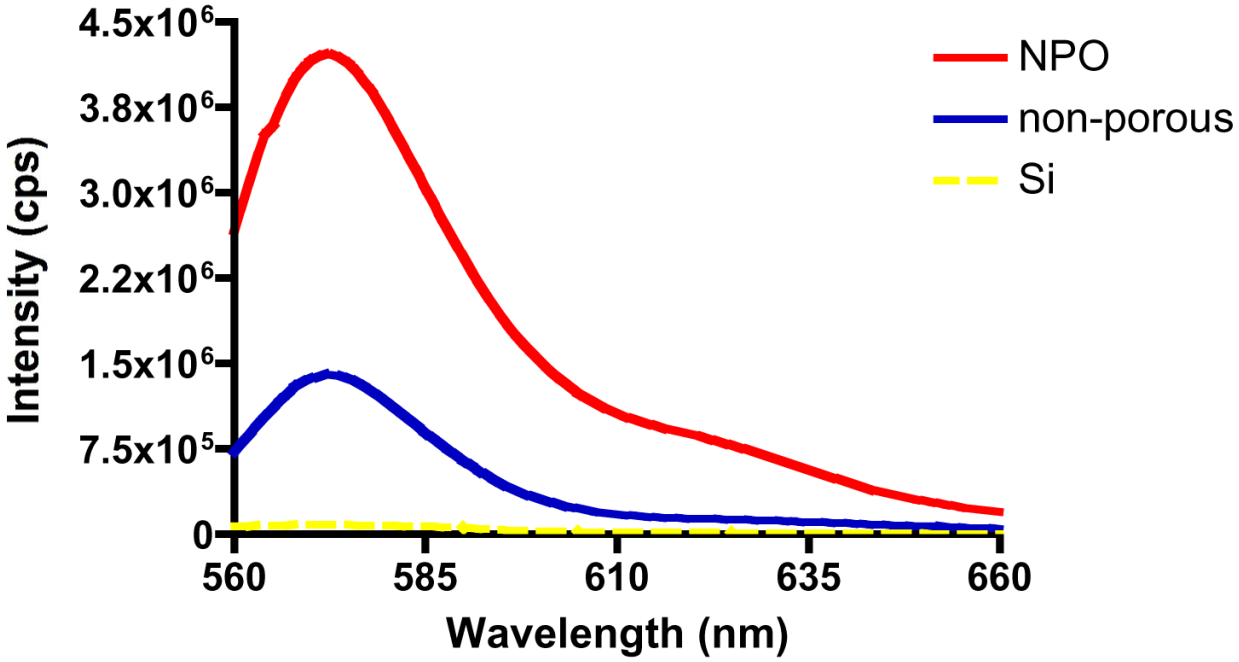

Fig. 2.
Comparison of fluorescence intensity from uncoated Si substrates (dotted yellow), coated with porous NPO (red), and coated with non-porous PMSSQ (blue).

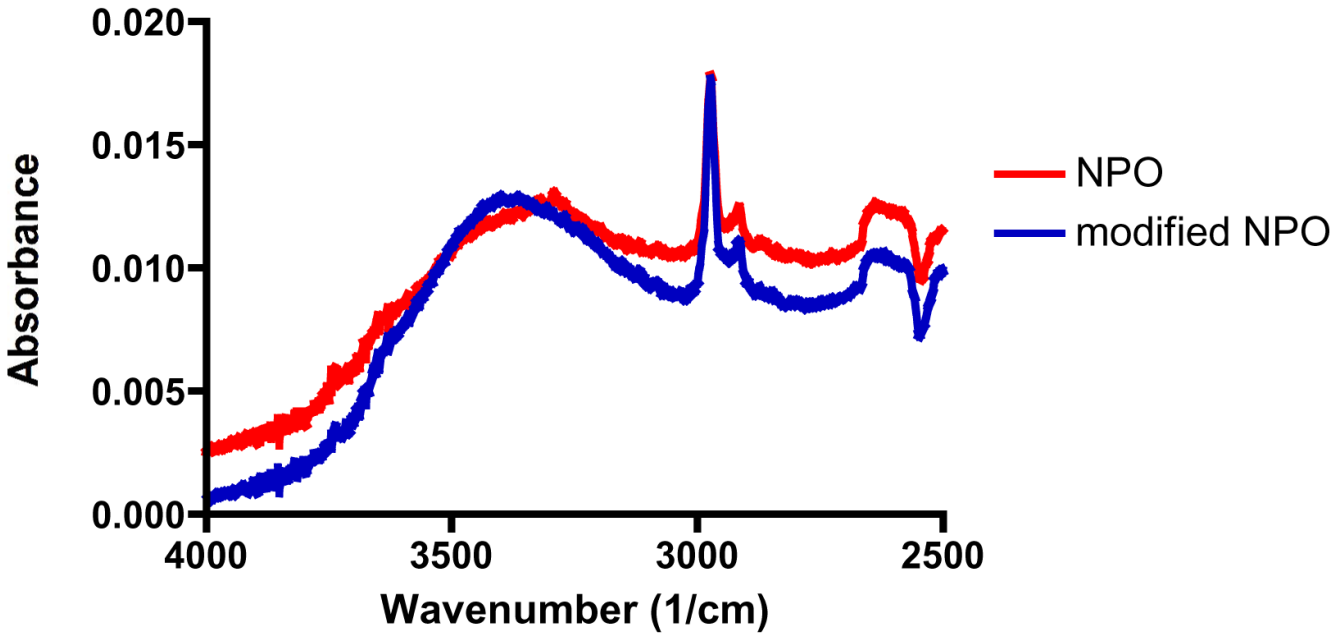

Fig. 3.
ATR FT-IR comparison of Si substrates with (blue) and without (red) modifications to the NPO surface coating.

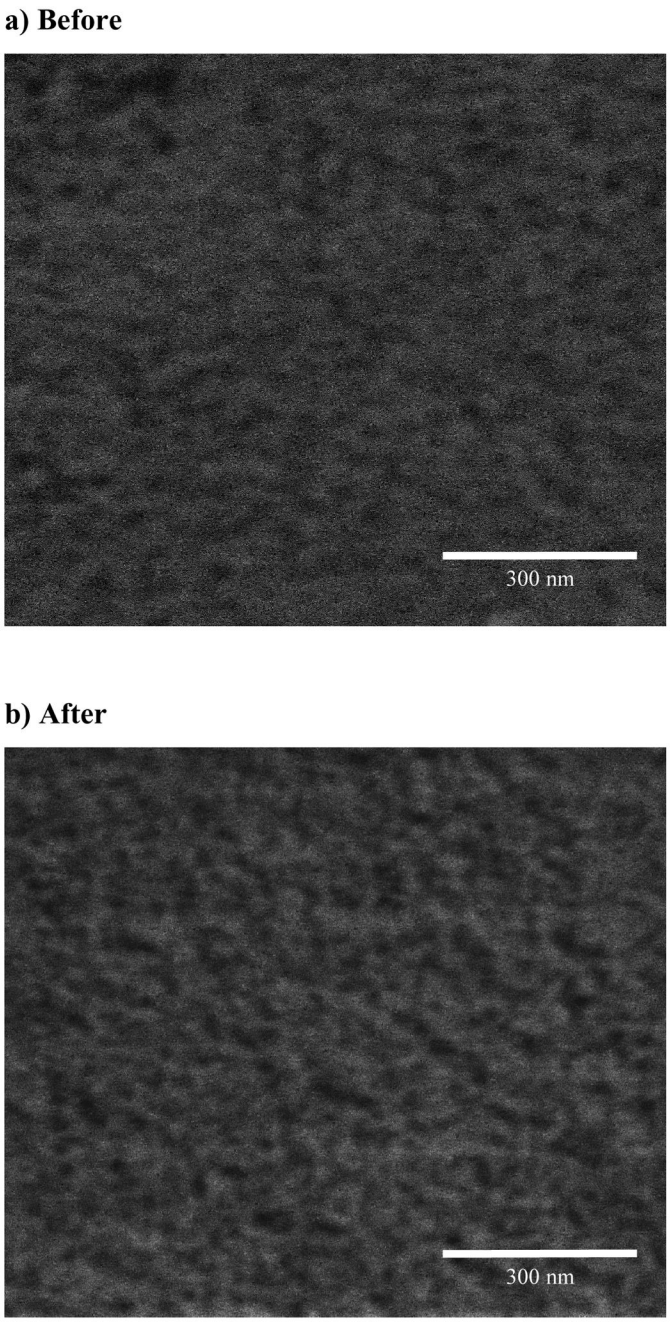

Fig. 4.
Scanning electron microscope images of NPO surface before (a) and after (b) surface modification with silanization, crosslinker application, and protein immobilization. Lighter regions represent NPO material while the darker spots represent pores within the material.

Table 1

Ellipsometry results for each NPO treatment step, with refractive indexes and layer thicknesses

		NPO layer	Modification layer
Oxygen/Plasma treated	***RI***	1.28	1.17
	Thickness (nm)	38.01	1358.9
Oxygen/Plasma treated, silanized and crosslinked	***RI***	1.28	1.175
	Thickness (nm)	30.956	1314.464
Oxygen/Plas ma treated, silanized, crosslinked, with protein	***RI***	1.46	1.19
	Thickness (nm)	16.698	1476.727